

Formation elastic parameters by deriving **S**-wave velocity logs

Colin C. Potter and Darren S. Foltinek

ABSTRACT

The calculation of the elastic parameters (Poisson's ratio, Bulk modulus, Rigidity modulus, Lamé's constant and Young's modulus) of a formation requires *P* sonic, *S* sonic and density logs. Where *S* sonic logs do not exist, they can be derived from a *P* sonic log and V_p/V_s ratios for each formation. The V_p/V_s values can be interpreted from other wells by statistical analysis of the V_p/V_s ratio of the formations in the region, predetermined values from lithology and *P*- and *S*-wave velocities from other analyses. Software to perform this calculation has been developed. Formation elastic parameters were calculated for four wells in the Blackfoot field in Southern Alberta. The elastic parameters allow further interpretation of the substructure. V_p/V_s , for example, has been shown to be a good indicator of lithology, including delineation of reservoir sands and shale content.

INTRODUCTION

Shear wave velocity logs combined with *P*-wave velocity logs and bulk density logs allows computation of elastic constants. Full-waveform and dipole logging tools provide both *P*-wave and *S*-wave sonic logs. However, these tools are not always used in boreholes and when they are used it is generally in the zone of interest. There always seems to be ample *P*-wave sonic and density logs, but not *S*-wave sonic logs. The recordings of *S*-waves combined with *P*-waves allow further rock property and elastic constant analysis. By estimating *S*-wave velocity logs, formation elastic parameters can be calculated and synthetic seismograms generated with the combination of *P*-wave sonic and density logs.

The ratio of compressional-wave velocity (V_p) to shear-wave velocity (V_s), or V_p/V_s gives additional information about lithology. Well log studies (Pickett, 1963; Nations, 1974; Kithas, 1976; Miller and Stewart, 1990) indicate a correlation between V_p/V_s values and lithology. Pickett (1963) established V_p/V_s values from core measurements of 1.9 for limestone, 1.8 for dolomite, and 1.6 to 1.75 for clean to calcareous sandstones.

By using predicted V_p/V_s values from lithologies and V_p/V_s values calculated from well logs, *S*-wave velocities can be estimated. Using the VPTOVS program (Foltinek et al., 1997) performs this estimation. The program calculates *S*-wave sonic logs from *P*-wave sonic logs using a depth variant V_p/V_s value or curve.

FORMATION ELASTIC PARAMETERS

Method

The first part of this study was to construct derived blocked logs of elastic parameters using the LOGEDIT algorithm (Foltinek et al., 1997). These parameters, in Table 3 – 6, are from four wells (PCP BLACKFOOT 8-8-23-23 (oil bearing sand channel), PCP 4B CAVALIER 4-16-23-23 (shale filled channel), PCP BLACKFOOT 12-16-23-23 (shale filled channel), and PCP BLACKFOOT 9-17-23-23 (regional)) all West of the 4th Meridian. These wells were selected because they have dipole sonic logs. The 08-08 and the 09-17 wells have dipole sonic logs from the Mannville to the Mississippian, while the 12-16 dipoles are from above Second White Speckled Shale to the Mississippian and the 04-16 well has dipoles from above the Bearpaw to the Mississippian or the length of the borehole.

From these four wells, the V_p/V_s ratios were calculated. The V_p/V_s ratios were blocked along with the P -wave sonic, S -wave sonic and bulk density curves. These curves were blocked using a mean value across lithological units. The units selected were based on previously defined horizons and the estimated bottom of the lithological units. These units allow a more accurate estimation of the V_p/V_s values than they would if the estimated bottoms were not included. The blocked P -wave sonic and S -wave sonic were converted to P -wave and S -wave velocities. These velocities and bulk density log values were used to calculate the V_p/V_s ratio, Poisson's ratio, Bulk modulus, Rigidity modulus, Lamé's constant and Young's modulus.

The equations for these calculations are as follows:

$$\mu = \rho \beta^2 \quad (1)$$

$$E = \rho \beta^2 ((3\alpha^2 - 4\beta^2) / (\alpha^2 - \beta^2)) \quad (2)$$

$$\sigma = (E - 2\mu) / 2\mu \quad (3)$$

$$\kappa = E / (3(1 - 2\sigma)) \quad (4)$$

$$\lambda = \kappa - 2\mu / 3 \quad (5)$$

where α or V_p is P -wave velocity (m/s); β or V_s is S -wave velocity (m/s); ρ is bulk density (kg/m³); σ is Poisson's ratio; κ is Bulk modulus (pascals); μ is Rigidity modulus (pascals); λ is Lamé's constant (pascals); E is Young's modulus (pascals).

Table 1 shows other relations for elastic constants in an isotropic media. Table 2 shows the naming conventions and lithologies for this paper. These data are provided for reference (revised from Potter et al., 1996) and the V_p/V_s values for use in the estimation of the S -wave velocity logs.

Observations

Tables 3 – 6 provide information to consider for the use of V_p/V_s values. In the 04-16 well, V_p/V_s is high in the Upper Cretaceous ranging from 1.92 for the Viking to

2.21 for the Belly River, suggesting high shale content. In the 04-16, 12-16 and 09-17 wells, values of 1.93 to 2.17 are reasonable for the coals. V_p/V_s for the Glauconitic channel top is lowest in the 08-08 (1.66) as compared to 12-16 (1.88) and 04-16 (1.92). This indicates higher porosity in the 08-08 well for the upper unit. In the lower sandstone unit, values of 1.65 and 1.67 are for the 08-08 and 12-16 wells, respectively. V_p/V_s for Sunburst are equal in the 04-16 and 09-17 at 1.91, indicating shale content. The Detrital V_p/V_s values range from 1.76 to 1.94 indicating lithological heterogeneity. The shaley carbonate Mississippian have values from 1.89 to 2.09.

ESTIMATING S-WAVE VELOCITY LOGS

Previous work has shown that V_p/V_s values change with lithology. V_p/V_s in mixed lithologies varies linearly between the limits of V_p/V_s for the end members (Nations, 1974; Kithas, 1976; Eastwood and Castagna, 1983; Rafavich et al., 1984; Wilkens, 1984; Castagna et al., 1985; Miller and Stewart, 1990). V_p/V_s values for different lithologies determined by Pickett (1963) and others are as follows: 2.0 – 2.5 for coal; 2.0 – 3.0 for shale; 1.9 for limestone; 1.8 for dolomite; 1.7 for calcareous sandstone; and 1.6 for clean sandstone. Ferguson and Stewart (1997) indicate V_p/V_s values of about 1.9 for the regional shales to about 1.7 for the glauconitic sands. These values are within the interpreted incised valley for the Blackfoot field. Reliable estimated V_p/V_s values were required for deriving S-wave sonics. The V_p/V_s values were interpolated from the dipole curves, the geology of the area (Miller et al., 1995) and predetermined lithology indicators as above.

Statistics and geostatistics

Statistics were obtained using ISATIS geostatistical software from Geovariances. Table 7 shows univariate statistics of the variables used from the four wells. The 64 samples are from each formation on all four wells. The V_p/V_s mean is 1.94 with a standard deviation of 0.14.

Correlation matrices were produced with different selection criteria. The variables used were V_p , V_s , V_p/V_s , density, Poisson's ratio, Bulk modulus, Rigidity modulus, Lamé's constant, Young's modulus, Bulk*density, Rigidity*density and lambda*density. The selections were all 64 samples or formation units, 52 samples that excluded coals and 55 samples of formation units from 2WS to Mississippian.

For all three selections, the maximum values did not change. The interesting change occurred when the coals were excluded. The minimum V_p and density increased. This caused every variable to increase as well, except V_s and Rigidity modulus that retained the same value. The minimum values for V_s and Rigidity are from the Belly River formation and have no effect whether there are coals or not. The V_p/V_s shows a better correlation with all variables, except Poisson's ratio.

Multi-linear regressions with 55 samples (from 2WS to Mississippian) for V_p/V_s with different variables gave constant coefficient values ranging from 1.94 to 2.02 with a mean of 1.92. This V_p/V_s average is very good for the lithological units. Figure 1 confirms these values with a V_p/V_s histogram. Figure 1 also shows the linear

relation of V_p to V_s in the second plot. The correlation of V_p to V_s has a high value of 0.93 or 93%. Figure 2 shows the V_p/V_s distribution relative to X coordinates, Y coordinates and subsea values or Kriging in 3-D.

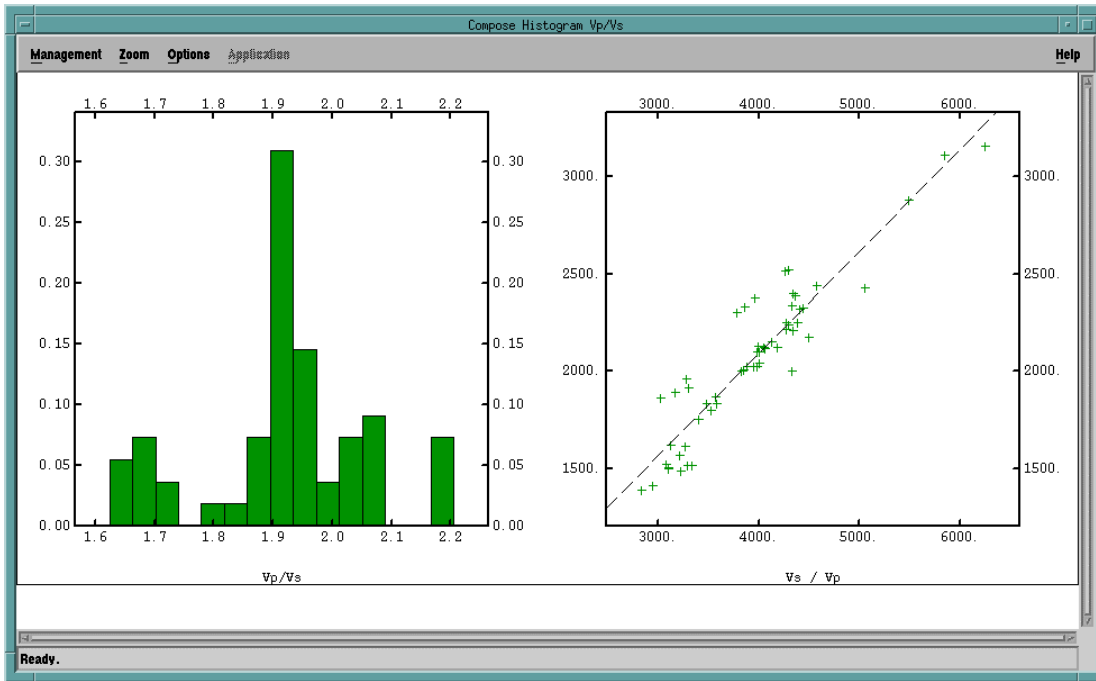


FIG. 1 V_p/V_s histogram and V_s versus V_p (m/s) for samples from 2WS to Mississippian.

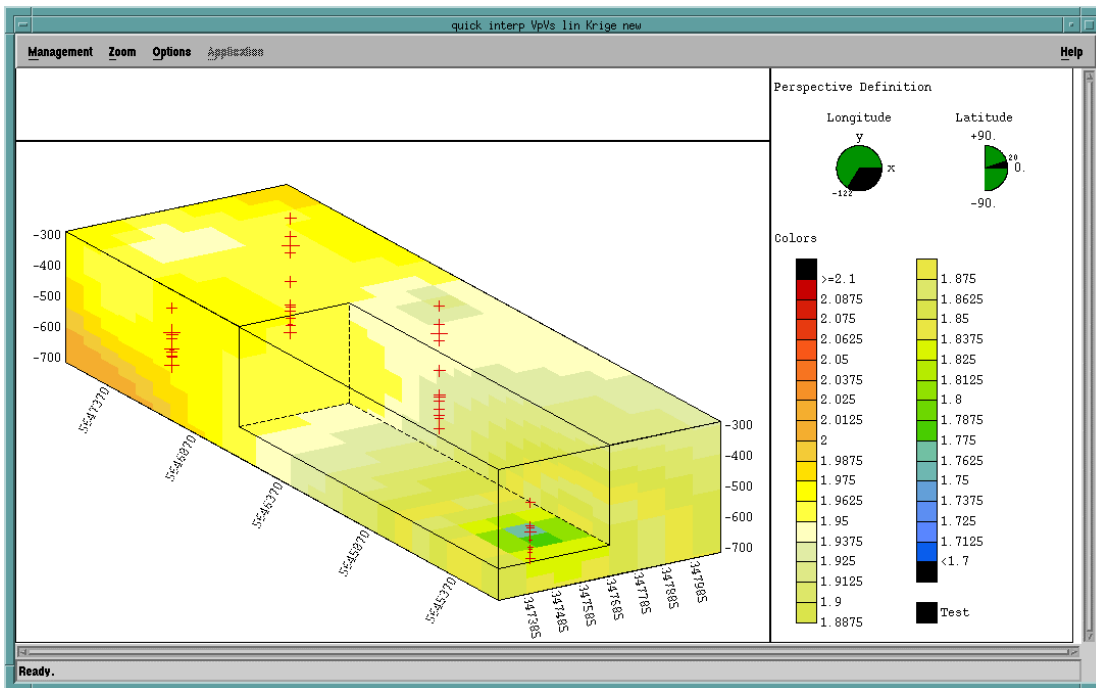


FIG.2 V_p/V_s values Kriged in 3-D.

Figure 2 shows low V_p/V_s values for the 08-08 well (near well) which is indicative of the oil bearing sand channel and higher values for the regional 09-17 well (far left). The 12-16 and 04-16 wells are second and third from the left, respectively.

Methods

By multiplying P -wave sonic logs with V_p/V_s logs or estimated V_p/V_s values, S -wave sonic logs are generated. These S -wave sonic logs are obtained using the VPTOVS (Foltinek et al., 1997) program (Figure 3). The V_p/V_s logs can either be blocked or unblocked.

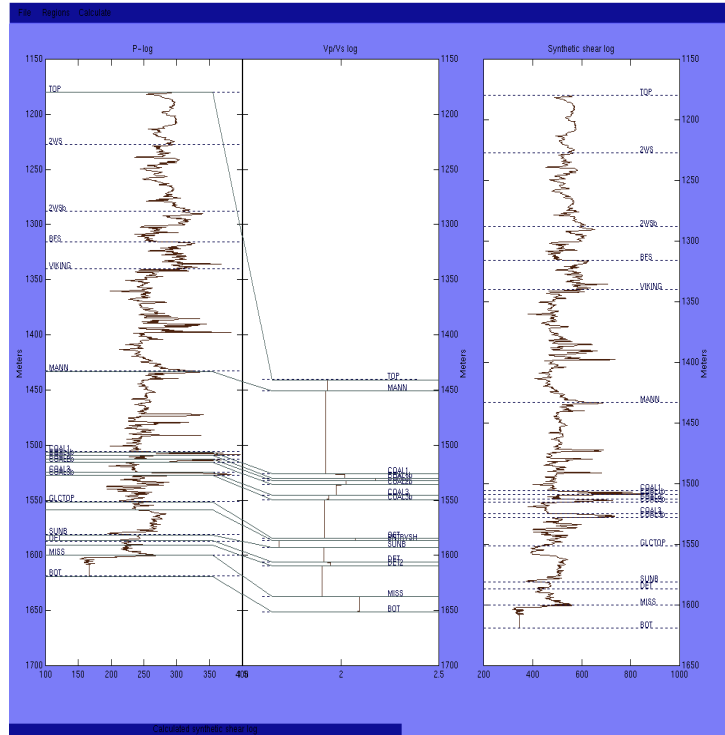


FIG.3. VPTOVS program interface.

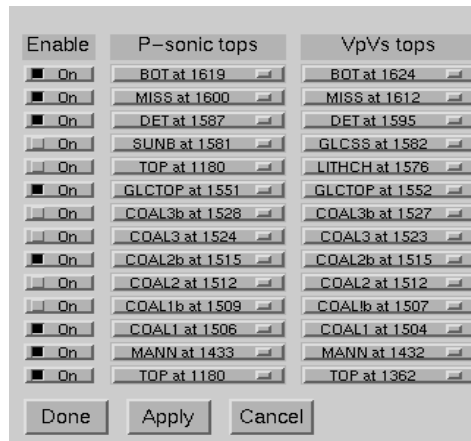


FIG. 4 Dialog box to match tops.

This program reads in a *P*-wave sonic, then a *Vp/Vs* curve. The unblocked *Vp/Vs* curve is blocked using a median value between units. The median filter was selected to provide accurate values in thin formation units (i.e. Coals) and to maintain the correct value when using blocked logs. The horizons or tops are defined across the two curves. The program attempts to match tops, by name, in the *P* sonic and the *Vp/Vs* curve. This produces the dialog box shown in Figure 4. The dialog box shows the correlation of similar horizons or tops and allows the interpreter to enable the matches. Once the tops are matched between the *P* sonic and *Vp/Vs* curve, a series of depth regions are defined in both curves (See Figure 5). For each region, *P* sonic values are multiplied by the median value of the *Vp/Vs* curve within that region to produce an *S*-wave sonic curve.

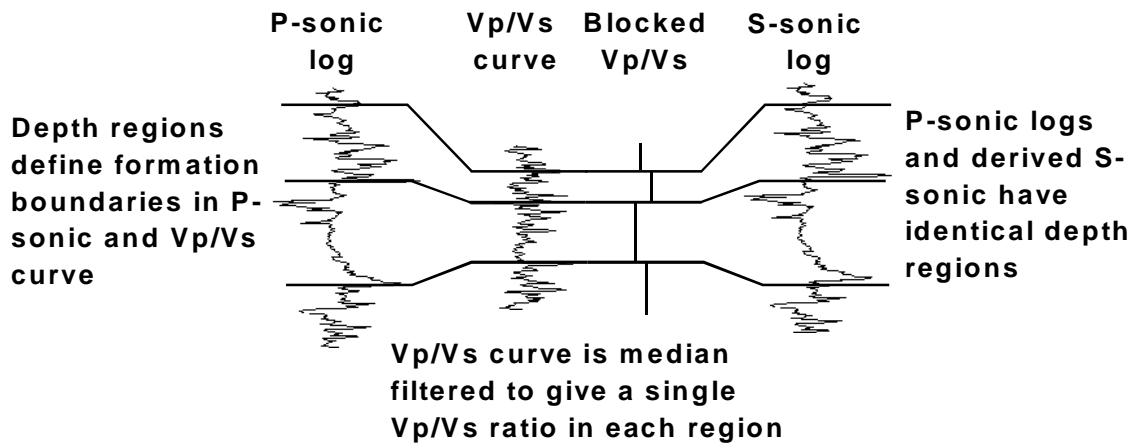


FIG. 5 Schematic showing relation of depth regions between logs.

In LOGEDIT, the dipole logs from four wells were separated into three geological categories, which are regional (09-17), shale-filled channel (04-16 and 12-16) and oil bearing sand channel (08-08). These logs were merged together depending on category and geological unit. The 04-16 curves are from above the Bearpaw to the Mississippian, so the top section was spliced on top of the other three curves depending on category. The merged curves are as follows: Regional – top of 04-16 on bottom of 09-17; Shale-filled channel – all of 04-16 and top of 04-16 on bottom of 12-16; Oil bearing sand channel – top of 04-16 correlated with 12-16 on top of 08-08.

Tops or formation names were edited on all logs in the Blackfoot area to have the same naming conventions (See Table 2). In VPTOVS, tops are moved primarily on the *P*-wave curve to adjust to varying unit and curve lengths. This program allows blocked *Vp/Vs* values to be edited at the interpreter's discretion.

Discussion

Figure 3 shows two logs of different lengths. This program allows different log lengths to be correlated to produce an *S*-wave sonic curve the same length as the input *P*-wave sonic curve. The program can be used as a fast way to estimate *S* sonic curves. The interpreter that has knowledge of the substructure and reliable *Vp/Vs*

values could benefit from the program. These values can be obtained from several different sources. The sources include shear wave sonics from full-waveform and dipole logging tools, predetermined lithological values, VSP surveys, *P-P* and *P-S* seismic inversions and even ground roll velocities. The program is most accurate using curves that match tops and lithology well.

By deriving the *S*-wave sonic, formation elastic parameters can be calculated providing a *P*-wave sonic and density curve is supplied. This rigorous approach could be integrated with other derivations of curves and velocities for a reliable interpretation of the substructure.

CONCLUSIONS

V_p/V_s values were calculated from *P*-wave sonic and *S*-wave sonic curves from four wells in the Blackfoot field. Formation elastic parameters were also calculated for the four wells using dipole sonic and density logs. When formation elastic parameters and elastic logs are generated, further interpretation of the substructure can be performed. Where *S* sonic curves do not exist, they can be derived from *P*-sonic curves and V_p/V_s curves or values. V_p/V_s come from wells where dipole or full-waveform sonics are available. V_p/V_s values used to derive *S*-wave sonics can be interpreted from other wells by statistical analysis of the V_p/V_s of the formations in the region predetermined values from lithology and *P*- and *S*-wave velocities from other analyses. The VPTOVS program was developed to derive *S*-wave sonic logs and gives a rigorous approach to deriving *S*-wave velocity logs.

FUTURE WORK

Analysis of formation elastic parameters for all wells from derived *S*-wave sonic logs would provide better diagnostic evaluation of the reservoir. The *S* sonic logs would produce *P-S* seismograms to correlate with *P-S* data sets. Inversion on the *P-S* surface seismic is needed to obtain *S*-wave velocities.

ACKNOWLEDGEMENTS

I would like to thank the staff of PanCanadian Petroleum Limited for valuable data and assistance of the project area, especially Jocelyn Dufour and Bill Goodway. I would also like to thank David Garner of TerraMod Consulting Inc. for providing the statistics and the CREWES staff for their assistance, in particular Henry Bland for his expert advice and computer knowledge.

REFERENCES

- Castagna, J.P., Batzle, M.L., and Eastwood, R.L., 1985, Relationships between compressional-wave and shear-wave velocities in clastic silicate rocks: *Geophysics*, 50, 571-581.
- Eastwood, R.L. and Castagna, J.P., 1983, Basis for interpretation of V_p/V_s ratios in complex lithologies: *Soc. Prof. Well Log Analysts 24th Annual Logging Symp.*
- Ferguson, R.J. and Stewart, R.R., 1997, Sand/shale differentiation using shear-wave velocity from *P-S* seismic data: Submitted to *J. Seis. Expl.*
- Foltinek, D.S., Margrave, G.F., Larsen, J.A., and Bland, H.C., 1997, 1997 CREWES software release: CREWES Research Report 1997, Ch 18.

- Kithas, B.A., 1976, Lithology, gas detection, and rock properties from acoustic logging systems: Soc. Prof. Well Log Analysts 17th Annual Symp.
- Miller, S.L.M., Aydemir, E.Ö. and Margrave, G.F., 1995, Preliminary interpretation of P-P and P-S seismic data from the Blackfoot broad-band survey: CREWES Research Report 1995, Ch 42.
- Miller, S.L.M. and Stewart, R.R., 1990, Effects of lithology, porosity and shaliness on P- and S-wave velocities from sonic logs: *Can. J. Expl. Geophys.*, 26, 94-103.
- Nations, J.F., 1974, Lithology and porosity from acoustic shear and compressional wave transit time relationships: Soc. Prof. Well Log Analysts 15th Annual Symp.
- Pickett, G.R., 1963, Acoustic character logs and their applications in formation evaluation: *J. Petr.Tech.*, June, 659-667.
- Potter, C.C., Miller, S.L.M., and Margrave, G.F., 1996, Formation elastic parameters and synthetic P-P and P-S seismograms for the Blackfoot field: CREWES Research Report 1996, Ch 37
- Rafavich, F., Kendall, C.H.St.C., and Todd, T.P., 1984, The relationship between acoustic properties and the petrographic character of carbonate rocks: *Geophysics*, 49, 1622-1636.
- Sheriff, R.E., 1991, *Encyclopedic Dictionary of Exploration Geophysics*, Third Ed., SEG
- Wilkens, R., Simmons, G., and Caruso, L., 1984, The ratio V_p/V_s as a discriminant of composition for siliceous limestones: *Geophysics*, 49, 1850-1860.

Table 1. Relations between elastic constants and velocities (Sheriff, 1991).

	Young's modulus, E	Poisson's ratio, σ	Bulk modulus, k	Shear modulus, μ	Lamé constant, λ	P-wave velocity, α	S-wave velocity, β	Velocity ratio, β/α
(E, σ)			$\frac{E}{3(1-2\sigma)}$	$\frac{E}{2(1+\sigma)}$	$\frac{E\sigma}{(1+\sigma)(1-2\sigma)}$	$\left[\frac{E(1-\sigma)}{(1+\sigma)(1-2\sigma)\rho}\right]^{1/2}$	$\left[\frac{E}{2(1+\sigma)\rho}\right]^{1/2}$	$\left[\frac{(1-2\sigma)}{2(1-\sigma)}\right]^{1/2}$
(E, k)		$\frac{3k-E}{6k}$		$\frac{3kE}{9k-E}$	$3k\left(\frac{3k-E}{9k-E}\right)$	$\left[\frac{3k(3k+E)}{\rho(9k-E)}\right]^{1/2}$	$\left[\frac{3kE}{(9k-E)\rho}\right]^{1/2}$	$\left(\frac{E}{3k+E}\right)^{1/2}$
(E, μ)		$\frac{E-2\mu}{2\mu}$	$\frac{\mu E}{3(3\mu-E)}$		$\mu\left(\frac{E-2\mu}{3\mu-E}\right)$	$\left[\frac{\mu(4\mu-E)}{(3\mu-E)\rho}\right]^{1/2}$	$\left(\frac{\mu}{\rho}\right)^{1/2}$	$\left(\frac{3\mu-E}{4\mu-E}\right)^{1/2}$
(σ, k)	$3k(1-2\sigma)$			$\frac{3k(1-2\sigma)}{2(1+\sigma)}$	$3k\left(\frac{\sigma}{1+\sigma}\right)$	$\left[\frac{3k(1-\sigma)}{\rho(1+\sigma)}\right]^{1/2}$	$\left[\frac{3k(1-2\sigma)}{2\rho(1+\sigma)}\right]^{1/2}$	$\left[\frac{1-2\sigma}{2(1-\sigma)}\right]^{1/2}$
(σ, μ)	$2\mu(1+\sigma)$		$\frac{2\mu(1+\sigma)}{3(1-2\sigma)}$		$\mu\left(\frac{2\sigma}{1-2\sigma}\right)$	$\left[\left(\frac{2\mu}{\rho}\right)\left(\frac{1-\sigma}{1-2\sigma}\right)\right]^{1/2}$	$\left(\frac{\mu}{\rho}\right)^{1/2}$	$\left[\frac{1-2\sigma}{2(1-\sigma)}\right]^{1/2}$
(σ, λ)	$\lambda\frac{(1+\sigma)(1-2\sigma)}{\sigma}$		$\lambda\left(\frac{1+\sigma}{3\sigma}\right)$	$\lambda\left(\frac{1-2\sigma}{2\sigma}\right)$		$\left[\left(\frac{\lambda}{\rho\sigma}\right)(1-\sigma)\right]^{1/2}$	$\left[\frac{\lambda(1-2\sigma)}{\rho(2\sigma)}\right]^{1/2}$	$\left[\frac{1-2\sigma}{2(1-\sigma)}\right]^{1/2}$
(k, μ)	$\frac{9k\mu}{3k+\mu}$	$\frac{3k-2\mu}{2(3k+\mu)}$			$k-2\mu/3$	$\left(\frac{k+4\mu/3}{\rho}\right)^{1/2}$	$\left(\frac{\mu}{\rho}\right)^{1/2}$	$\left(\frac{\mu}{k+4\mu/3}\right)^{1/2}$
(k, λ)	$9k\left(\frac{k-\lambda}{3k-\lambda}\right)$	$\frac{\lambda}{3k-\lambda}$		$\frac{3}{2}(k-\lambda)$		$\left(\frac{3k-2\lambda}{\rho}\right)^{1/2}$	$\left[\frac{3(k-\lambda)}{2\rho}\right]^{1/2}$	$\left[\frac{1}{2}\left(\frac{k-\lambda}{k-2\lambda/3}\right)\right]^{1/2}$
(μ, λ)	$\mu\left(\frac{3\lambda+2\mu}{\lambda+\mu}\right)$	$\frac{\lambda}{2(\lambda+\mu)}$	$\lambda+\frac{2}{3}\mu$			$\left(\frac{\lambda+2\mu}{\rho}\right)^{1/2}$	$\left(\frac{\mu}{\rho}\right)^{1/2}$	$\left(\frac{\mu}{\lambda+2\mu}\right)^{1/2}$
(α, β)	$\rho\beta^2\left(\frac{3\alpha^2-4\beta^2}{\alpha^2-\beta^2}\right)$	$\frac{\alpha^2-2\beta^2}{2(\alpha^2-\beta^2)}$	$\rho\left(\alpha^2-\frac{4}{3}\beta^2\right)$	$\rho\beta^2$	$\rho(\alpha^2-2\beta^2)$			

Table 2. Formation naming conventions and lithologies.

Abbreviation	Unit Name	General Lithology
BRPAW	Bearpaw	Shale
BR	Belly River	Sandstone/Siltstone
BRSS	Belly River Sandstone	Sandstone
OLDMAN	Oldman	Sandstone/Coal
FOREMOST	Foremost	Sandstone/Coal
PAKOW	Pakowki	Shale
BBR	Basal Belly River	Shale
MILKR	Milk River	Sandstone/Gas
1WS	First White Speckled Shale	Shale
2WS	Second White Speckled Shale	Shale/Gas/Oil
2WSb	Second White Speckled Shale Base	Shale
BFS	Base of Fish Scales Zone	Shale
VIKING	Viking	Sandstone/Gas/Oil
MANN	Upper Mannville	Sandstone/Siltstone/Shale
COAL1	1st Coal Layer	Coal
COAL1b	1st Coal Layer Base	Sandstone
COAL2	2nd Coal Layer	Coal
COAL2b	2nd Coal Layer Base	Sandstone
COAL3	3rd Coal Layer Base	Coal
COAL3b	3rd Coal Layer Base	Sandstone
GLCTOP	Glauconitic Channel Top	Sandstone/Gas/Oil
LITHCH	Lithic Channel Unit	Lithic Sandstone
GLCSS	Glauconitic Channel Porous Sandstone	Sandstone/Oil
OST	Ostracod	Limestone/Gas/Oil
BNTRYSH	Bantry Shale	Shale
SUNB	Sunburst	Sandstone
DET	Detrital	Sandstone/Siltstone/Shale
DET2	2nd Detrital	Sandstone/Siltstone/Shale
MISS	Shunda – Mississippian	Carbonate

Table 3. Formation parameters for 08-08.

Formation	Subsea	V_p	V_s	V_p/V_s	σ	ρ	κ	μ	λ	E
Units	m	m/s	m/s	-	-	Kg/m ³	e10Pa	e10Pa	e10Pa	e10Pa
MANN	-513.9	3978	2097	1.897	0.308	2512	2.502	1.105	1.765	2.890
COAL1	-585.9	3022	1859	1.625	0.195	1944	0.879	0.672	0.431	1.607
COAL1b	-588.9	4327	2329	1.858	0.296	2596	2.983	1.408	2.044	3.650
COAL2	-593.9	3303	1909	1.730	0.249	2073	1.254	0.755	0.751	1.887
COAL2b	-596.9	4337	2391	1.814	0.282	2563	2.868	1.465	1.891	3.755
COAL3	-605.9	3159	1889	1.672	0.222	2145	1.120	0.765	0.610	1.870
COAL3b	-608.9	4185	2119	1.976	0.328	2539	2.928	1.139	2.168	3.026
GLCTOP	-634.9	3860	2322	1.662	0.216	2412	1.859	1.300	0.992	3.163
LITHCH	-658.9	4299	2513	1.710	0.240	2530	2.544	1.598	1.479	3.964
GLCSS	-663.9	3783	2295	1.648	0.209	2383	1.736	1.255	0.899	3.035
DET	-676.9	4409	2506	1.759	0.261	2521	2.790	1.583	1.734	3.994
MISS	-693.9	5844	3100	1.885	0.304	2645	5.645	2.541	3.951	6.629

Table 4. Formation parameters for 09-17.

Formation	subsea	V_p	V_s	V_p/V_s	σ	ρ	κ	μ	λ	E
Units	m	m/s	m/s	-	-	Kg/m ³	e10Pa	e10Pa	e10Pa	e10Pa
MANN	-513.1	3874	2019	1.919	0.314	2529	2.421	1.031	1.733	2.709
COAL1	-588.1	3071	1520	2.021	0.338	2157	1.370	0.498	1.038	1.333
COAL1b	-592.1	4324	1994	2.169	0.365	2624	3.516	1.044	2.821	2.849
COAL2	-594.1	3260	1611	2.024	0.339	2252	1.615	0.584	1.225	1.564
COAL2b	-598.1	4340	2203	1.970	0.327	2596	3.210	1.260	2.370	3.342
COAL3	-608.1	3115	1615	1.929	0.316	2216	1.380	0.578	0.995	1.521
COAL3b	-612.1	4002	2092	1.914	0.312	2600	2.648	1.137	1.890	2.984
OST	-647.1	4494	2169	2.072	0.348	2576	3.587	1.212	2.779	3.268
BNTYSH	-649.1	3276	1954	1.677	0.224	2378	1.341	0.908	0.736	2.222
SUNB	-655.1	4050	2117	1.913	0.312	2551	2.660	1.143	1.898	3.000
DET	-669.1	3396	1749	1.941	0.319	2431	1.812	0.744	1.316	1.963
DET2	-672.1	4274	2245	1.903	0.309	2549	2.942	1.285	2.086	3.365
MISS	-700.1	5058	2422	2.088	0.351	2669	4.741	1.566	3.698	4.232

Table 5. Formation parameters for 12-16.

Formation	subsea	V_p	V_s	V_p/V_s	σ	ρ	κ	μ	λ	E
Units	m	m/s	m/s	-	-	Kg/m ³	e10Pa	e10Pa	e10Pa	e10Pa
2WS	-303.4	3583	1831	1.957	0.323	2496	2.089	0.837	1.531	2.214
2WSb	-363.4	3524	1795	1.963	0.325	2469	2.006	0.795	1.475	2.108
BFS	-391.4	3335	1512	2.205	0.371	2390	1.929	0.546	1.564	1.498
VIKING	-415.4	3846	2002	1.921	0.314	2513	2.374	1.008	1.702	2.648
MANN	-509.4	4003	2037	1.965	0.325	2524	2.647	1.048	1.949	2.777
COAL1	-581.4	3099	1502	2.063	0.347	2032	1.340	0.458	1.035	1.234
COAL1b	-585.4	4297	2230	1.927	0.316	2582	3.055	1.284	2.199	3.379
COAL2	-587.4	3205	1565	2.047	0.343	2144	1.501	0.525	1.151	1.411
COAL2b	-591.4	4576	2434	1.880	0.303	2608	3.402	1.546	2.371	4.027
COAL3	-600.4	3097	1497	2.068	0.347	1962	1.295	0.440	1.002	1.185
COAL3b	-603.4	4269	2207	1.934	0.318	2575	3.021	1.254	2.185	3.305
GLCTOP	-628.4	3988	2122	1.879	0.303	2559	2.532	1.152	1.764	3.001
GLCSS	-649.4	3961	2372	1.670	0.220	2370	1.940	1.334	1.051	3.255
DET	-652.4	4401	2314	1.901	0.309	2571	3.143	1.377	2.225	3.605
MISS	-674.4	6254	3148	1.987	0.330	2674	6.927	2.650	5.161	7.050

Table 6. Formation parameters for 04-16.

Formation	subsea	V_p	V_s	V_p/V_s	σ	ρ	κ	μ	λ	E
Units	m	m/s	m/s	-	-	Kg/m ³	e10Pa	e10Pa	e10Pa	e10Pa
BRPAW	597.6	2954	1358	2.175	0.366	2290	1.435	0.422	1.153	1.154
BR	464.6	2960	1339	2.210	0.371	2100	1.337	0.377	1.086	1.033
BRSS	447.6	3131	1580	1.982	0.329	2168	1.404	0.541	1.043	1.439
OLDMAN	400.6	3356	1646	2.039	0.342	2288	1.750	0.620	1.337	1.664
FOREMOST	354.6	3215	1487	2.161	0.364	2288	1.690	0.506	1.352	1.381
BBR	152.6	3232	1504	2.150	0.362	2444	1.817	0.553	1.449	1.505
PAKOW	128.6	3082	1432	2.152	0.362	2433	1.646	0.499	1.313	1.359
MILKR	103.6	3597	1864	1.930	0.317	2503	2.079	0.870	1.499	2.290
1WS	11.6	3537	1813	1.952	0.322	2522	2.051	0.829	1.498	2.190
2WS	-302.4	3562	1864	1.911	0.312	2548	2.053	0.885	1.463	2.321
2WSb	-360.4	3482	1828	1.905	0.310	2510	1.925	0.839	1.366	2.198
BFS	-390.4	3291	1516	2.171	0.365	2475	1.923	0.569	1.544	1.553
VIKING	-413.4	3826	1995	1.918	0.313	2513	2.346	1.000	1.679	2.626
MANN	-508.4	3982	2020	1.972	0.327	2517	2.623	1.027	1.938	2.725
COAL1	-586.4	2939	1410	2.085	0.351	2018	1.209	0.401	0.941	1.084
COAL1b	-589.4	3950	2018	1.957	0.323	2531	2.575	1.031	1.888	2.729
COAL2	-593.4	3223	1487	2.168	0.365	2157	1.606	0.477	1.288	1.301
COAL2b	-595.4	4378	2246	1.950	0.322	2596	3.231	1.309	2.358	3.460
COAL3	-605.4	2825	1385	2.040	0.342	1978	1.073	0.379	0.820	1.018
COAL3b	-608.4	4127	2144	1.925	0.315	2599	2.835	1.194	2.039	3.142
GLCTOP	-636.4	4053	2110	1.921	0.314	2574	2.701	1.146	1.937	3.011
SUNB	-655.4	4442	2321	1.913	0.312	2563	3.215	1.381	2.295	3.625
DET	-665.4	4360	2381	1.831	0.287	2515	2.879	1.427	1.928	3.673
MISS	-699.4	5492	2870	1.914	0.312	2402	4.607	1.978	3.288	5.191

Table 7. Statistics for 64 formation units.

VARIABLE	Min	Max	Mean	Std.Dev.	Variance	Skew	Kurtosis
UTMX	347522	347949	347771	196.4991	38611.90	-0.4363	1.1633
UTMY	5645335	5647386	5646659	756.2254	571876.91	-0.6221	-31.0983
Depth SS	-700.12	597.59	-456.353	325.5905	106009.18	1.9600	5.6177
KB	918.13	938.6	929.3656	8.1791	66.90	0.0062	1.3302
Depth TVD	327	1638	1385.718	327.3325	107146.58	-1.9619	5.6195
V_p	2825	6254	3833.14	689.8387	475877.46	1.0865	4.7107
V_s	1339	3148	1987.89	403.5491	162851.85	0.5178	3.2744
V_p/V_s	1.625	2.21	1.9440	0.1440	0.02073	-0.2971	2.8311
σ	1944	2674	2421.75	195.4463	38199.25	-1.0052	2.8286
ρ	0.1950	0.3710	0.3134	0.0422	0.00178	-1.1556	3.8393
κ	0.8792	6.9270	2.3941	1.0745	1.15459	1.7004	7.2903
μ	0.3765	2.6496	1.0170	0.4699	0.22078	1.0817	4.9354
λ	0.4311	5.1606	1.7161	0.8074	0.65192	1.7004	7.3754
E	1.0180	7.0500	2.6579	1.2154	1.47725	1.1831	5.3447
Formation Int	1	30	17.8125	7.4831	55.996	-0.2734	2.4510